axial methyl. The 1,2 diequatorial substitution thus seems to be a factor leading to skew-boat features in the conformation.

V. Conclusion

The development of a new parameter set including gauche interactions, which reflect molecular distortions from idealized geometry, is an improvement over the previous set, which only involved positional methyl substitutions. The new approach is used to predict chemical shifts for the same methylcyclohexanes with chair conformations along with the decalins and methylcyclohexanes with significant steric distortions to the chair conformation. In addition to a wider applicability, the new parameter set uses only 14 parameters, instead of the 18 used in the previous set.

Acknowledgment. This research was supported in part by the National Institutes of Health under Grant No. 5 R01 GM08521-28 and by the U.S. Air Force under Grant No. F 33615-86-C-2643.

Supplementary Material Available: Tables of coefficients for multiple stepwise linear regression with explicit distortion and associated structures of compounds (24 pages). Ordering information is given on any current masthead page.

^{15}N Chemical Shifts of Backbone Amides in Bovine Pancreatic Trypsin Inhibitor and Apamin

John Glushka, Maria Lee, Scott Coffin, and David Cowburn*

Contribution from The Rockefeller University, 1230 York Avenue, New York, New York 10021.
Received March 10, 1989

Abstract: ^{15}N chemical shifts of backbone amides were measured at natural abundance for apamin and bovine pancreatic trypsin inhibitor using heteronuclear multiquantum proton-detected correlated spectroscopy (HMP-COSY). Chemical shift differences from values expected for random-coil peptides were calculated and examined with respect to structural features, including torsion angles and intramolecular hydrogen bonds. A correlation with the torsion angle Ψ_{i-1} was observed for the β-sheet residues. No other dominant factor was found to account for the large (up to ± 15 ppm) variation from the model peptides. The results suggest that these ^{15}N shifts are sensitive to nonbonded interactions, though there is no systematic variation with respect to a single structural parameter.

Empirical correlations between molecular structure and ^{15}N chemical shifts continue to pose a challenge.[2,3] An important question is whether ^{15}N chemical shift data can provide information about the environments of backbone amides or side chains in a protein that would contribute to understanding its three-dimensional structure. Although current methods for calculating solution structures of proteins and nucleic acids rely primarily on distances from nuclear Overhauser effects, additional geometric constraints derived from chemical shifts could aid the computation or increase the confidence in the final structures obtained. In addition, the study of molecular interactions will be aided by the rationalization of chemical shift changes that are observed.

Analyses of gramicidin,[4] oxytocin,[5] aluminochrome,[6] vancomycin,[7] and actinomycin,[8] for example, have shown that changes in solvent and hydrogen bonding have large effects on ^{15}N chemical shifts. The importance of the latter effect has been also discussed theoretically.[9] A correlation between van der Waals interactions and chemical shifts of second-row elements is consistent with many β and γ effects.[10] Work on homopolypeptides in the solid state has revealed a small but significant downfield shift of amide signals in β sheets relative to α-helix structures.[11]

The recent application of proton-detected heteronuclear correlated spectroscopy and isotope labeling to proteins[12] has provided a growing list of chemical shift data for backbone amides and side-chain nitrogens. To date, spectra that give at least some residue-type assignments have been obtained from proteins such as bovine pancreatic trypsin inhibitor (BPTI),[13] *Staphylococcus* nuclease,[14] thioredoxin,[15] T4 lysozyme,[16,17] *Salmonella* phage P22 c2 repressor,[18] fl coat protein,[19] *Anabena* flavodoxin,[20] turkey ovomucoid third domain,[21] λ *cro* repressor, and others.[22] Residues

(1) This paper is dedicated to the memory of the late Emil Thomas Kaiser (1938-1988).
(2) Levy, G. C.; Lichter, R. L. In *Nitrogen-15 NMR Spectroscopy*; Wiley-Interscience: New York, 1979.
(3) Witanowski, M.; Stefaniak, L.; Webb, G. A. *Annu. Rev. NMR Spectrosc.* **1986**, *18*, 65-191.
(4) Live, D. H.; Davis, D. G.; Agosta, W. C.; Cowburn, D. *J. Am. Chem. Soc.* **1984**, *106*, 1939-1941.
(5) Live, D. H.; Wyssbrod, H. R.; Fischman, A. J.; Agosta, W. C.; Bradley, C. H.; Cowburn, D. *J. Am. Chem. Soc.* **1979**, *101*, 474-479.
(6) Llinas, M.; Horsley, W. J.; Klein, M. P. *J. Am. Chem. Soc.* **1976**, *98*, 7554.
(7) Hawkes, G. E.; Molinari, H.; Singh, S. *J. Magn. Reson.* **1987**, *74*, 188-192.
(8) Juretsche, H. P.; Lapidot, A. *Eur. J. Biochem.* **1984**, *143*, 651-658.
(9) Prado, F. R.; Giessner-Prettre, C.; Pullman, A.; Hinton, J. F.; Harpool, D.; Metz, K. R. *Theor. Chim. Acta* **1981**, *59*, 55-69.
(10) Li, S.; Chesnut, D. B. *Magn. Reson. Chem.* **1985**, *23*, 625-638.
(11) Shoji, A.; Ozaki, T.; Fujito, T.; Deguchi, K.; Ando, I. *Macromolecules* **1987**, *20*, 2441-2445.
(12) Griffey, R. K.; Redfield, A. G. *Q. Rev. Biophys.* **1987**, *19*, 51-82.
(13) Glushka, J.; Cowburn, D. *J. Am. Chem. Soc.* **1987**, *109*, 7879-7881.
(14) Torchia, D. A.; Sparks, S. W.; Bax, A. *Biochemistry* **1988**, *27*, 5135-5141.
(15) LeMaster, D. M.; Richards, F. M. *Biochemistry* **1985**, *24*, 7263-7268.
(16) McIntosh, L. P.; Dahlquist, F. W.; Redfield, A. G. *J. Biomol. Struct. Dynam.* **1987**, *5*, 21-34.
(17) McIntosh, L. P.; Griffey, R. H.; Muchmore, D. C.; Nielson, C. P.; Redfield, A. G.; Dahlquist, F. W. *Proc. Natl. Acad. Sci. U.S.A.* **1987**, *84*, 1244-1248.
(18) Senn, H.; Eugster, A.; Otting, G.; Suter, F.; Wüthrich, K. *Eur. Biophys. J.* **1987**, *14*, 301-306.
(19) Schiksnis, R. A.; Bogusky, M. J.; Tsang, P.; Opella, S. J. *Biochemistry* **1987**, *26*, 1373-1381.
(20) Stockman, B. J.; Westler, W. M.; Mooberry, E. S.; Markley, J. L. *Biochemistry* **1988**, *27*, 136-142.

0002-7863/89/1511-7716$01.50/0

of the same type show chemical shift differences of up to 30 ppm, and values of 5–10 ppm are common. These large variations in chemical shifts are strikingly different from those measured in smaller peptides. This might be explained in part by the reduced averaging of shifts in the proteins due to a smaller conformer population, by unusual bond angles and strong internal hydrogen bonding, or by the greater number of nonbonded interactions in closely packed domains of larger proteins. The third possibility is supported by observations of increasing deviations in predicted shifts of homopolypeptides as the bulkiness of the side chains increases.[23] Lack of accurate structural information for these larger proteins has so far precluded an analysis of this ^{15}N shift information. To begin this analysis, one accessible approach is to look for dominant effects which might be reflected in torsion angles or hydrogen bond patterns of smaller, well-described proteins.

Bovine pancreatic trypsin inhibitor (BPTI), a 58-residue protein, has been widely used for a variety of NMR studies.[24-27] X-ray crystal structures[28-30] and an NOE-derived solution structure[31] are available. Apamin, an 18-residue neurotoxin from honey bee venom, has a well-defined helical section and a β-turn, stabilized by two disulfide linkages, as determined by a number of NMR investigations.[32-35] In addition, exchange rates of certain hydrogens measured over a pH range suggest formation and destabilization of hydrogen bonds, with a possible conformational change.[33]

Materials and Methods

BPTI (Trasylol) was a gift from Bayer AG. A 23-mmol solution in 90% H_2O/10% D_2O was adjusted to pH 3.5 and 4.6 with HCl and NaOH solutions. Spectra were obtained at 50 and 68 °C, respectively.

Apamin was purchased from Sigma. A 15-mmol solution in 90% H_2O/10% D_2O was adjusted to pH values of 2.2, 3.4, and 4.0. For a 2 M salt solution, NaCl was added directly to the sample at pH 4.0.

N-Acetyl amino acids were obtained commercially, and solutions were made in DMSO, except for histidine and arginine, which were measured in water.

Spectra were obtained on a GN-500 spectrometer with probes built by GE NMR instruments or by Cryomagnetic, Inc., with inner proton coils and separate outer broad-band coil.[36] Double-quantum-filtered COSY spectra were obtained in the standard way, with preirradiation to saturate the water peak.[37] INEPT pulse sequences were used to obtain spectra of the *N*-acetyl amino acids, and heteronuclear multiple-quantum proton-detected HMP-COSY's were used to obtain ^{15}N spectra of the proteins. The latter pulse sequences were either the most basic version without nitrogen decoupling, phase cycled for either zero- or double-quantum frequencies,[38] incorporating a Redfield selective pulse to avoid excitation of the water resonance,[39] or a decoupled refocused sequence using the spin echo selective pulse.[40] Data were typically processed with a Gaussian function in t_2 and zero filling in t_1. Further details are included with the appropriate figures.

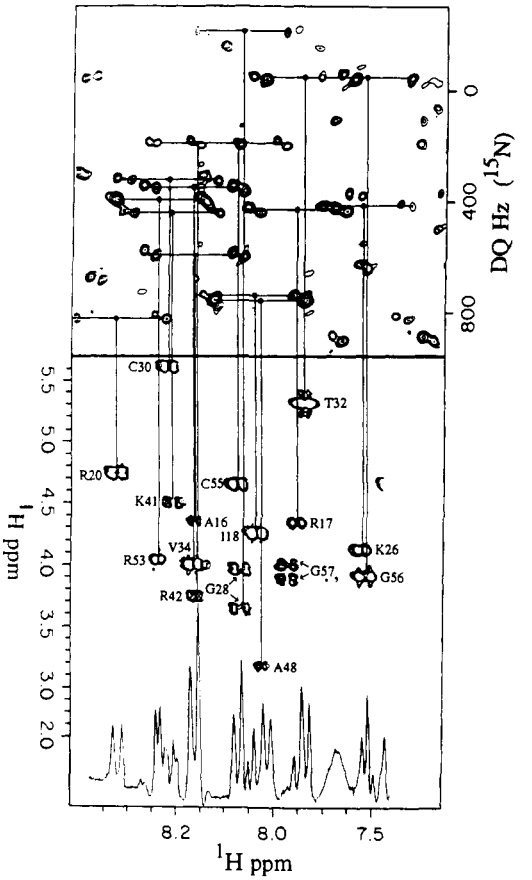

Figure 1. Portion of the amide region of a double-quantum HMP-COSY spectrum of BPTI, 23 mmol, pH 4.6, 68 °C with a corresponding region of α-H, NH cross peaks from a 2QF-COSY spectrum. The HMP-COSY spectrum was obtained with a Redfield selective pulse[39] to avoid excitation of the water resonance. The data matrix was 4096 by 128 with acquisition times of 680 and 16 ms for t_1 and t_2, respectively. For each block, 1200 accumulations were taken, with an interacquisition delay of 100 ms for a total accumulation time of 33 h. The spectrum is presented in absolute value mode. No decoupling of nitrogen was done, so COSY cross peaks were connected to the center of the doublets. The additional splitting of each peak in the doublet derives from homonuclear $^3J(H^\alpha-H')$. The phase-sensitive 2QF-COSY spectrum in this figure was processed with a final magnitude calculation, so the cross-peak patterns are not resolved.

Results

Assignments of amide nitrogens were obtained by cross-correlating peaks from the HMP-COSY contour plots to known proton assignments (see Figure 1). The BPTI proton data were taken from two lists, with sample conditions at 68 °C, pH 4.6,[25] and 35 °C, pH 3.5.[24] Spectral regions were clarified by comparing data directly to phase-sensitive double-quantum-filtered COSY spectra taken with the same sample. For most of the residues, the data at 68 °C were sufficient for assignment. In some cases the lower temperature spectrum provided additional data from rapidly exchanging amides, as well as corroborating the previous assignments. Only small chemical shift changes were observed between the two data sets, and so, for the purposes of the structural analysis, the data were combined.

The full list of chemical shift data for BPTI appears in Table I. Although most of the assignments were unequivocal, some very crowded regions and weak signals allowed only tentative

(21) Oritz-Polo, G.; Krishnamoorthi, R.; Markley, J. L.; Live, D. H.; Davis, D. G.; Cowburn, D. *J. Magn. Reson.* **1986**, *68*, 303–310.
(22) Leighton, P.; Lu, P. *Biochemistry* **1987**, *26*, 7262–7271.
(23) Kricheldorf, H. R.; Hull, W. E. *Org. Magn. Reson.* **1979**, *12*(11), 607–611.
(24) Pardi, A.; Wagner, G. Wüthrich, K. *Eur. J. Biochem.* **1983**, *137*, 445–454.
(25) Wagner, G.; Wüthrich, K. *J. Mol. Biol.* **1982**, *155*, 347–366.
(26) Tüchsen, E.; Woodward, C. *J. Mol. Biol.* **1985**, *185*, 405–419.
(27) Tüchsen, E.; Woodward, C. *J. Mol. Biol.* **1985**, *185*, 421–430.
(28) Deisenhofer, J.; Steigmann, W. *Acta Crystallogr.* **1975**, *B31*, 238–250.
(29) Wlodawer, A.; Walter, J.; Huber, R.; Sjölin, L. *J. Mol. Biol.* **1984**, *180*, 301–329.
(30) Wlodawer, A.; Nachman, J.; Gilliland, G. L.; Gallagher, W.; Woodward, C. *J. Mol. Biol.* **1987**, *196*, 611–639.
(31) Wagner, G.; Braun, W.; Havel, T. F.; Schaumann, T.; Go, N.; Wüthrich, K. *J. Mol. Biol.* **1987**, *196*, 611–639.
(32) Wemmer, D.; Kallenbach, N. R. *Biochemistry* **1983**, *22*, 1901–1906.
(33) Dempsey, C. F. *Biochemistry* **1986**, *25*, 3904–3911.
(34) Pease, J. H. B.; Wemmer, D. E. *Biochemistry* **1988**, *27*, 8491–8498.
(35) Bystrov, V. F.; Okhanov, V. V.; Miroshnikov, A. I.; Ovchinnikov, Y. A. *FEBS Lett.* **1980**, *119*, 113–117.
(36) Live, D. H.; Davis, D. G.; Agosta, W. C.; Cowburn, D. *J. Am. Chem. Soc.* **1984**, *106*, 6104–6105.
(37) Rance, M.; Sørensen, O. W.; Bodenhausen, G.; Wagner, G.; Ernst, R. R.; Wüthrich, K. *Biochem. Biophys. Res. Commun.* **1983**, *117*, 479–485.
(38) Bax, A.; Griffey, R. H.; Hawkins, B. L. *J. Magn. Reson.* **1983**, *55*, 301.
(39) Redfield, A. G.; Kunz, S.; Hurd, T. *J. Magn. Reson.* **1975**, *19*, 114–117.
(40) Sklenar, V.; Bax, A. *J. Magn. Reson.* **1987**, *74*, 469–479.

Table I. Chemical Shifts of ^{15}N Resonances in BPTI

residue	δ^1H^a	$\delta^{15}N^b$	$\Delta\delta^{15}N^c$	residue	δ^1H^a	$\delta^{15}N^b$	$\Delta\delta^{15}N^c$	residue	δ^1H^a	$\delta^{15}N^b$	$\Delta\delta^{15}N^c$	residue	δ^1H^a	$\delta^{15}N^b$	$\Delta\delta^{15}N^c$
D3	8.49	123.6[d,e]	+1.5	R20	8.33	129.8	+0.7	F33	9.32	119.4	−4.9	K46	9.71	120.5[e]	−5.5
F4	7.57	115.9	−6.9	Y21	9.10	115.9	−8.0	V34	8.17	118.9	−2.8	S47	7.46	103.0	−14.5
C5	7.37	120.9	−0.2	F22	9.74	120.2	−2.6	Y35	9.26	129.9	+4.5	A48	8.03	125.6	−1.5
L6	7.50	114.2	−9.6	Y23	10.46	125.1	+1.2	G36	8.49	114.1	+1.9	E49	8.48	119.8[d]	−0.8
E7	7.50	120.8	−1.7	N24	7.78	125.8	+2.1	G37		[f]		D50	7.72	120.0	−2.1
Y10	7.64	123.1	−0.8	A25	8.59	126.8	+0.6	C38	7.74	115.2	−4.0	C51	6.95	119.8	−1.3
T11	8.74	127.3[e]	+14.9	K26	7.82	116.7	−7.4[e]	R39	8.92	113.5[e]	−12.6	M52	8.50	121.3	−0.8
G12	7.00	107.1	−5.6	A27	6.77	118.5	−7.7	A40	7.30	118.3	−7.9	R53	8.25	120.5	−6.1
C14	8.54	117.9[d]	−3.2	G28	8.07	106.9	−2.4	K41	8.22	121.2	+2.9	T54	7.38	113.5	+1.1
K15	7.83	115.5[d,e]	−9.5	L29	6.76	114.6	−7.3	R42	8.15	115.8	−10.8	C55	8.09	114.8	−7.8
A16	8.17	123.7	−2.5	C30	8.23	118.8	−2.3	N43	7.22	116.4	−7.3	C56	7.82	107.8	−3.4
R17	7.95	118.3	−6.4	Q31	8.74	123.2	−1.0	N44	6.73	121.3	−2.4	G57	7.98	108.8[d,e]	−1.9
I18	8.04	125.3	+2.3	T32	7.94	108.9	−3.5	F45	9.85	122.6	−0.2	A58	7.72	129.5	+5.2
I19	8.46	128.4	+2.9												

[a] Chemical shifts of amide protons at 68 °C, pH 4.6, relative to TSP, taken from ref 25. [b] Chemical shifts relative to anhydrous NH_3, calculated from internal TSP and external $MeNO_2$. [c] Structural chemical shift differences, $\delta^{15}N_{residue} - \delta^{15}N_{random\ coil}$, where $\delta^{15}N_{random\ coil} = \delta^{15}N_{N\text{-acetyl amino acid}} + \Delta\delta^{15}N_{NRC\ and\ solvent\ change}$. A positive number indicates a downfield shift relative to the "random-coil" model. [d] These assignments are considered tentative, due to proton overlap of C14, E49, and D3, and the absence of D3 at 68 °C, pH 4.6. [e] Observed only at lower temperatures (50 °C, pH 3.5, or 35 °C pH 4.6). [f] G37 has been assigned upfield at 4.3 ppm[58] and could not be observed with the selective pulse used in the HMP-COSY experiment.

Table II. Chemical Shifts of ^1H and ^{15}N Resonances of Apamin

	δ^1H^a				$\delta^{15}N^b$				
residue	pH 2.2	pH 3.4	pH 4.0	pH 4.0 with 2 M NaCl	pH 2.2	$\Delta\delta^{15}N^c$	pH 3.4	pH 4.0	pH 4.0 with 2 M NaCl
Cys-1									
Asn-2	9.14	9.67	10.14	9.65	127.4	(+4.6)	128.7	129.6	128.5
Cys-3	9.02	8.99	8.98	8.86	120.5	(+0.1)	120.4	120.0	119.8
Lys-4	8.05	8.02	8.03	8.02	119.8	(−5.5)	119.6	119.4	119.7
Ala-5	7.23	7.19	7.18	7.16	119.9	(−3.2)	119.9	119.8	119.2
Pro-6									
Glu-7	9.12	9.86	10.52	9.89	122.2	(+0.7)	123.3	124.0	123.8
Thr-8	7.38	7.30	7.20		107.4	(−3.9)	106.5	105.8	
Ala-9	8.96	8.97	9.00	8.92	126.5	(+2.8)	126.2	125.9	126.9
Leu-10	8.30	8.26	8.25	8.26	119.4	(−3.6)	119.5	120.0	119.8
Cys-11	7.78	7.84	7.93	7.83	117.1	(−3.1)	117.7	117.2	116.8
Ala-12	8.47	8.42	8.40	8.42	123.5	(+1.2)	123.2	122.8	123.1
Arg-13	7.99	7.96	8.00	8.02	117.5	(−8.2)	117.7	117.6	117.6
Arg-14	8.26	8.28	8.34	8.40	120.7	(−2.5)	121.1	120.9	120.8
Cys-15	8.41	8.42	8.48	8.51	116.7	(−3.6)	116.9	116.7	116.4
Gln-16	7.68	7.73	7.72	7.70	119.4	(−3.1)	119.2	119.0	119.2
Gln-17	7.95	7.93	7.93	7.92	119.5	(−3.5)	119.3	118.9	118.6
His-18	8.31	8.28	8.24	8.15	119.6	(−8.7)	119.3	118.6	118.4

[a] Chemical shifts relative to TSP. [b] Chemical shifts relative to anhydrous NH_3, calculated from internal TSP and external $MeNO_2$. [c] Chemical shift differences from random-coil models calculated for the data from pH 2.2, as explained in the text.

assignments. These include C14, D3, E49, K15, and G57.[41] In some cases, Q31, for example, the $^3J_{HH}$ fine structure provided additional data that supported the assignment. For V34, A16, and R42, which are overlapping in the proton dimension at 68 °C, pH 4.5, the small changes for these peaks under different conditions allowed their assignment.

Similarly, the apamin proton data were taken from Wemmer and Kallenbach[32] and supplemented by Dempsey,[33] Bystrov et al.,[35] and COSY spectra. A typical $^1H\{^{15}N\}$-correlated spectrum is shown in Figure 2. Table II summarizes the ^1H and ^{15}N chemical shift data for three pH values and for a sample with high ionic strength.

^{15}N chemical shifts of amides in "random-coil" peptides were approximated by using *N*-acetyl amino acids in DMSO, which reflect the primary effects of the side chain and the peptide linkage on the amide chemical shift.[5] However, corrections had to be made for the flanking residues on both the amide and carboxyl ends, as well as the solvent change. The neighboring residue corrections were estimated from values reported by Kricheldorf for oligopeptides in DMSO and water.[42] That analysis led to a few general observations: (1) All amino acids cause downfield shifts with respect to Gly, i.e., for peptides of the type X-Gly-Gly. (2) Glycine causes upfield shifts in peptides Gly-Y-Y. (3) Neighboring residue effects become larger with increasing bulkiness of the side chain, i.e., Ala < Leu < Val < Ile. However, variations in very similar compounds provide many exceptions.[42] For example, Z-Gly-Pro-Leu-Leu-OMe and Z-Gln-Leu-Leu-OMe show a difference of 0.7 ppm in the Leu-OMe amides. This suggests that either effects from more than one residue away are important (on the order of 1 ppm) or that random coil is not an accurate term even for these simple tripeptides. Variations in the neighboring residue effects depend on the peptide and the solvent as well. For example, in going from –Gly-Gly*– to –Met-Gly*–, the Gly* experiences a shift of +2.1 ppm, due to the Met residue. However, a compound containing –Gly-Val–, when compared to –Met-Val–, shows a shift of +0.5 ppm for the Val residue that is due to the Met residue. Additionally, the same residue in the same set of peptides will experience different shifts on the order of 1–2 ppm, depending on the solvent.[42]

Therefore, it was necessary to average the available data, and approximate neighboring group corrections that could be applied to each residue in the protein were obtained. The amino acids were grouped into four main classes: (1) glycine and alanine (though the neighboring group effects vary from 0 to 0.5 ppm,[42] they were not considered significant for this analysis), (2) leucine and other amino acids with methylene at the β position, (3) valine, and (4) isoleucine. These classes reflect the major effect on a peptide amide due to the groups at the α and β positions of the preceding residue. Other effects, such as charged side chains, polar functional groups at the β carbon, and aromatic groups, were not separately analyzed due to insufficient data. Though these groups

(41) The assignments of E49 and C14 in ref 13 should be reversed. This change is based on the pH sensitivity of E49 (see ref 24). The similar chemical shift values for these two residues do not affect the analysis.

(42) Kricheldorf, H. R. *Org. Magn. Reson.* **1981**, *15*, 162–177.

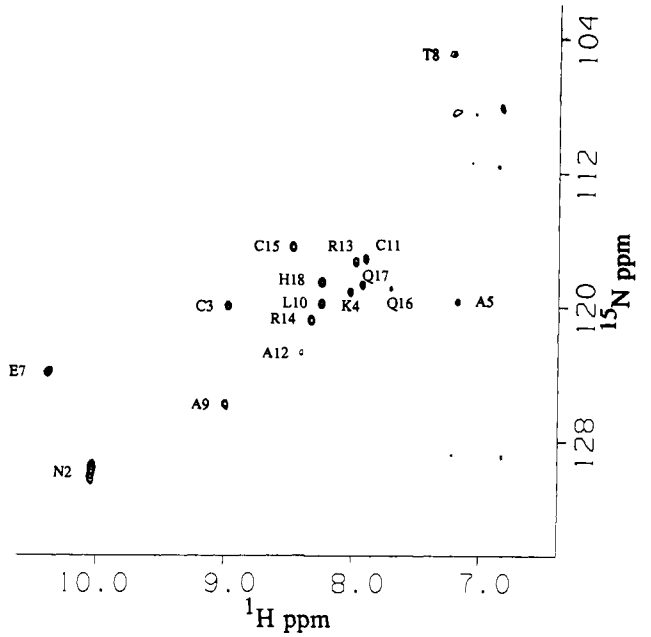

Figure 2. HMP-COSY spectrum of apamin, 15 mmol, pH 4.0, 25 °C. A 1-1 spin-echo sequence was used to avoid excitation of the water resonance[40] and appropriate phase cycling implemented to allow decoupled, pure absorption peaks. The data were collected in a 1024 × 128 matrix and processed with a Gaussian function applied to t_2 and a shifted sine bell and zero-filling applied to t_1 to give a final matrix of 1024 × 512.

may play an important role when secondary structure affects their proximity to a particular amide, it was assumed that the side chains would be extended in the model peptides and functional groups beyond the β carbon would be less important. The limited data available also did not clarify the effect of proline, and so it was grouped with the β methylene residues. The neighboring residue corrections (NRC = $\delta_{x-y} - \delta_{Ac-y}$, where y is the observed residue, x is the substituted residue, and Ac refers to the *N*-acetyl group of the model compound) derived are the following: (1) for glycine and alanine, −5.5 ppm; (2) for leucine and other β methylene side chains, including threonine and proline, −3.6 ppm; (3) for valine, −2.1 ppm; (4) for isoleucine, −1.1 ppm. The limited available data showed that the change from a free carboxyl in DMSO to an ester appeared to be less than 1 ppm, and so this correction was not used in the analysis. In addition, a correction for solvent change from DMSO to H_2O was required. These values were estimated by averaging reported values of alanyl, glycyl, and valyl residues in both DMSO, water, and formic acid, which gives similar chemical shifts as water.[42] The values for alanyl and glycyl residues ranged from +2.2 to +5.1 ppm, and the values for valyl residues ranged from +5.1 to +8.5 ppm, with the averages being +4 and +6 ppm, respectively. All amino acid residues with β-methylene side chains were then assumed to be affected in the same degree, and, similarly, isoleucyl residues were expected to experience the same solvent shift as valyl residues. It is possibe that bulky hydrophobic side chains as in tryptophan may behave more like valine than the leucine. The effect of a polar β substituent, such as the threonine hydroxyl, for example, was treated simply as a β methylene. In a comparison of ^{15}N chemical shifts of an insulin derivative in water and DMSO, differences of 3–4 ppm were observed for all residues, including valine.[43] However, the full and unambiguous assignment of the insulin spectra was lacking and so the data from the peptide work were considered more reliable. The sum of all corrections then provided random-coil values for all residues in a specified peptide fragment. Because of the approximations discussed, the analysis of secondary structural effects in relation to the models is probably valid only for larger (>3 ppm) chemical shift differences.

(43) Hull, W. E.; Bullesbach, E.; Wieneke, H.-J.; Zahn, H.; Kricheldorf, H. R. *Org. Magn. Reson.* **1981**, *17*(2), 92–96.

Table III. ^{15}N Chemical Shifts of *N*-Acetyl Amino Acids[a] and Random-Coil Peptides[b]

		neighboring residue$_{i-1}$			
residue$_i$	*N*-acetyl	Gly,Ala	β-methylene[c]	Val	Ile
Ala	125.7	125.3	127.2	130.6	131.6
Arg	125.5	124.9	126.8	128.3	129.3
Asn	123.2	122.6	124.5	126.0	127.0
Asp	121.6	121.0	122.9	124.4	125.4
Cys	120.6	120.0	121.9	123.4	124.4
Gln	123.7	123.1	125.0	126.5	127.5
Glu	122.0	121.4	123.3	124.8	125.8
Gly	110.7	110.1	112.0	113.5	111.5
His	128.9	128.3	130.2	131.7	132.7
Ile	120.6	121.9	123.8	125.3	126.3
Leu	123.3	122.7	124.6	126.1	127.1
Lys	131.2	130.6	132.5	134.0	135.0
Met	121.6	121.0	122.9	124.4	125.4
Phe	122.3	121.7	123.6	125.1	126.1
Pro	132.1	131.5	133.4	134.9	125.9
Ser	117.0	116.4	118.3	119.8	120.8
Thr	111.9	111.3	113.2	114.7	115.7
Trp	123.6	123.0	124.9	125.8	127.4
Tyr	123.4	122.8	125.7	126.2	127.2
Val	119.3	120.6	122.5	124.0	125.0

[a] *N*-Acetyl amino acids in DMSO, ppm relative to NH_3. [b] Random-coil peptides in H_2O, ppm relative to NH_3. [c] All residues containing a side-chain β-methylene, i.e., Asp, Asn, Glu, Gln, Arg, Lys, Phe, Tyr, Trp, His, Leu, Ser, Thr, Pro, Met, Cys.

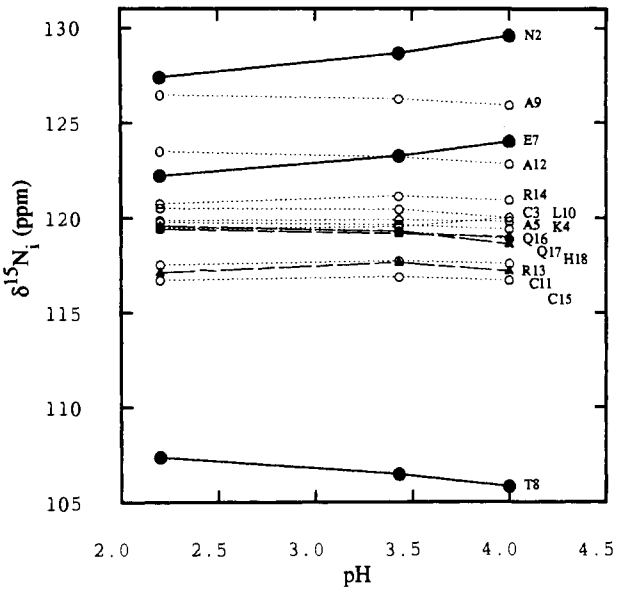

Figure 3. Plot showing change of $\delta^{15}N$ of amide nitrogens in apamin at three pH values. Filled circles indicate residues that experienced significant chemical shift changes; filled triangles (C11, Q16, H18) represent those residues that were expected to change their hydrogen bond strength but did not undergo significant chemical shift changes. (See text and Table II.)

Table III lists the calculated random-coil chemical shifts assigned to all residue pairs. The difference between the observed and calculated random-coil shift provided the chemical shift difference value, $\Delta\delta^{15}N$. A positive value indicates that the amide nitrogen signal has shifted downfield. Table I includes the chemical shift differences for BPTI, and Table II shows the values calculated for apamin at pH 2.2.

In addition to comparison ^{15}N chemical shifts of proteins to model compounds, a study of the chemical shift changes associated with proposed hydrogen bond changes was also undertaken. Studies of proton-exchange rates and chemical shifts on apamin have indicated that two hydrogen bonds form from amide donors, E7 and N2, as the E7 side-chain carboxyl titrates (pK_a 3.6), and hydrogen bonds from C11, Q16, and T8 amides destabilize over the pH range 2–5.[33] Figure 3 shows the change of ^{15}N chemical shifts over this pH range. As the pH increased, E7 and N2 amide

signals were shifted downfield by 1.8 and 2.2 ppm, respectively, and T8 shifted upfield by 1.6 ppm. The addition of 2 M NaCl to the sample at pH 4.0 caused an upfield shift of 1.1 ppm for N2, a downfield shift of 1.0 ppm for A9, and an upfield shift of 0.7 ppm for A5. No significant shifts were observed for E7 or other amide nitrogens.

Discussion

The range of chemical shift differences observed is approximately ±15 ppm for BPTI and +3 to −8 ppm for apamin, similar to what has been observed for other proteins. It is substantially larger than the range of deviations expected from ring current shifts.[44-48] Unexpectedly, there appears to be a greater number of upfield shifts in the observed data relative to the model compound data. It is possible that this bias stems from inadequacies in the calculated random-coil values and is not an indication of some physical phenomenon. The variations in the corrections to the random-coil models, for example, may account for a 1-2 ppm downfield bias in the model. The relative values, however, are more important for a structural analysis, and no attempt was made to readjust the model values to reflect a better "average". As mentioned in the introduction, analysis of these values was restricted to an empirical approach that examined structural parameters such as hydrogen bonding and torsion angles. Though a thorough analysis requires a multifactorial approach, this preliminary investigation sought first to determine any dominant factors by assessing independently each possible variable.[49]

Unlike the results from solid homopolypeptides, the residues in the β sheet of BPTI (residues A16-R20 and N24-L29) did not show any overall downfield shifts relative to α-helical regions in either BPTI (residues C51-A58) or apamin (residues A9-H18) (see Tables I and II).

Hydrogen Bonding. In a protein such as BPTI, individual peptides generally have a combination of interresidue, residue–solvent hydrogen bonds, and interresidue bonds mediated by internal water molecules. Strong intramolecular hydrogen bonds with favorable geometry would be expected to have a greater deshielding effect over the more transient solvent hydrogen bonds. A qualitative estimate of the degree of hydrogen bonding for a particular amide was determined from the particular bonding scheme indicated by crystal structure I (nearly identical with structures II and III) and supporting ^{1}H NMR evidence.[30] This basic information was supplemented qualitatively by amide proton to carbonyl–oxygen distances,[24] amide proton-exchange kinetics,[50] solvent accessibility,[26,50] and other indicators of hydrogen bond stability as defined by H-bond length fluctuations[51] or rate of D_2O exchange. A preliminary assessment of the role of hydrogen bonding was to compare the $\Delta\delta^{15}$N values with the amide proton chemical shift variations discussed by Pardi et al.[24] The authors established a cube root distance dependence for chemical shifts of protons in hydrogen bonds and attributed this to electric field effects, local magnetic anisotropies, and polarization of the ^{1}H electron cloud due to the proximity of the oxygen. There is little correspondence to the nitrogen shifts, except in a few areas, most notably residues 25–32 and less clearly for residues 7–14 and 34–38. Residues 25–32 represent most of the turn and part of one side of the β sheet.

Table IV. Hydrogen Bonding Patterns for the β-Sheet Region of BPTI

residue$_i$	hydrogen bonding[a] NH_i donor	hydrogen bonding[a] CO_{i-1} acceptor	solvent accessibility[b] NH	solvent accessibility[b] CO	exchange rate[c]	$\Delta\delta^{15}$N[d]
A16	un		1.6		87	−2.5
R17			4.8		*f*	−6.4
I18	un, lo		0.0		6.5	+2.3
I19		st, sh	3.6	0.0	*f*	+2.9
R20	st		0.0		7.1	+0.7
Y21	st, sh	st, sh	0.0		5.6	−8.0
F22	st, sh	st, sh	0.0		5.9	−2.6
Y23	st, sh	st, sh	0.0		6.2	+1.2
N24	st		0.0		12	+2.1
A25		st, sh	1.8	0.0	*f*	+0.6
K26			0.5	0.76	*f*	−7.4
A27	lo		0.0	1.03	~320	−7.7
G28	st		0.4		52	−2.4
L29	lo		0.0		9.6	−7.3
C30		st, sh	1.0	0.0	*f*	−2.3
Q31	st, sh		0.0		11	−1.0
T32		st, sh	3.6	0.0	210	−3.5
F33	sh		0.0		6.8	−4.9
V34		st, sh	4.6	0.0	140	−2.8
Y35	sh, st	sh	0.0	0.0	10	+4.5
G36	st	un, sh	0.0		50	+1.9

[a] Key: (i) "st" and "un" indicate stable and unstable hydrogen bonds, respectively, according to Levitt.[51] "Stable" hydrogen bonds were considered <1.90 Å with an rms length fluctuation <0.22 Å. (ii) "sh" and "lo" indicate short and long hydrogen bonds, respectively, according to Pardi et al.[24] Short hydrogen bonds were considered <2 Å with the amide proton shifted downfield from a random-coil model. [b] Solvent accessibility defined as $(A/4\pi r^2)100$, where A is the portion of an atom's vdW surface accessible to a spherical solvent molecule of radius 1.4 Å. Values for NH are from ref 50, and values for CO are from ref 27. [c] Exchange rates K_m in 10^{-3} min^{-1} for 68 °C, pH 3.5, from ref 50. The letter "f" (fast) indicates the amide proton exchanged too rapidly to be observed in the COSY spectrum at 10 °C. [d] Chemical shift differences, 68 °C, pH 4.6, from Table I.

For further analysis, the peptides were separated into broad classes of hydrogen bonding patterns, as described by crystal structure I.[24,28] Amides were grouped according to whether they acted as donors in an H bond and whether the adjacent carbonyl accepted one or more hydrogen bonds from either NH or CH protons. There is no clear correlation between downfield shifts and intramolecular hydrogen bonding as defined by this classification, probably because of the presence of solvent.[52] Attempts to restrict the analysis to small subsets of residues and to further characterize the hydrogen bonds did not lead to any clear correlations. For example, examination of Table IV shows that residues Y21, F22, Y23, and Y35 have very similar types of hydrogen bonds, amide proton-exchange rates, and solvent accessibility, yet their $\Delta\delta^{15}$N values range from −8 to +4.5 ppm. Including buried water molecules in the hydrogen bonding patterns did not significantly alter the results.

A similar comparison of the apamin data (pH 2.2) to random-coil chemical shift values reveals the same wide variation. For example, A9 ($\Delta\delta^{15}$N = +2.8) and A12 ($\Delta\delta^{15}$N = +1.2) are both downfield, which is compatible with participation in multiple hydrogen bonds, either as donors or bonded to acceptor carbonyls.[33,53] However, R13, C11, L10, and Q16 all have similar hydrogen bond patterns and yet are all relatively upfield. R13 in particular is a donor amide and the preceding carbonyl of A12 is an acceptor, yet it is 8.7 ppm upfield of its random-coil value.

More promising results were obtained from the comparison of chemical shifts at different pH values. The significant downfield shift of E7 and N2 amides (Table II and Figure 3) was compatible

(44) McDonald, C. C.; Philips, W. D. *J. Am. Chem. Soc.* **1967**, *89*, 6337.
(45) Sternlicht, H.; Wilson, D. *Biochemistry* **1967**, *6*, 2881–2892.
(46) Cowburn, D.; Bradbury, E. M.; Crane-Robinson, C.; Gratzer, W. B. *Eur. J. Biochem.* **1970**, *14*, 83–93.
(47) Perkins, S. J.; Wüthrich, K. *Biochem. Biophys. Acta* **1979**, *576*, 409–423.
(48) Redfield, C.; Hoch, J. C.; Dobson, C. M. *FEBS Lett.* **1983**, *159*, 132–136.
(49) A linear regression analysis was done on the chemical shift data from BPTI using crystal structure I values. Using different numbers of variables, including classes of hydrogen bonds, functions of torsion angles, and, in some cases, presence of neighboring groups, correlation matrices were calculated with either the observed chemical shifts or the calculated chemical shift differences as the dependent variable. In all the calculations, only the Ψ_{i-1} function gave any significant correlation value (0.5). Because of the small data set and many variables, errors were large in all the calculations, and the analysis did not reveal any information different than that obtained from inspection.
(50) Wagner, G.; Wüthrich, K. *J. Mol. Biol.* **1982**, *160*, 343–361.
(51) Levitt, M. *Nature* **1981**, *294*, 379–380.
(52) Supplementary material, Figure s-2.
(53) Sherman, S. A.; Andrianov, A. M.; Akhrem, A. A. *Dokl. Biophys.* **1987**, *293*, 48–51.

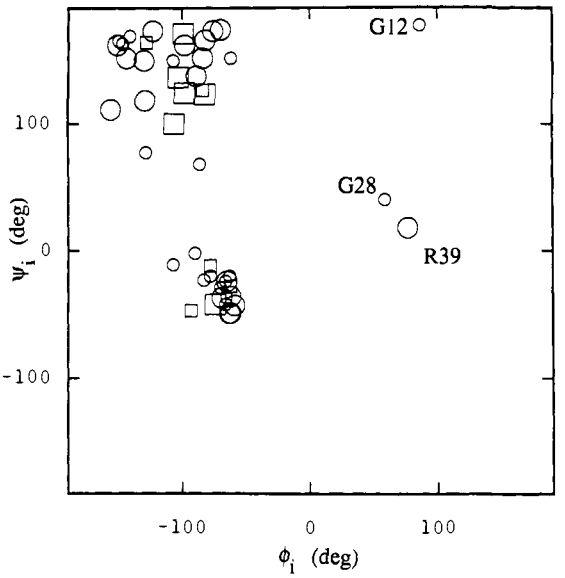

Figure 4. ^{15}N shift deviations superimposed on a Ramanchandran plot of BPTI ϕ and Ψ angles from crystal structure I.[28] The chemical shift differences have been grouped into four ranges: large □, >+2; □, 0–2 ppm; O, <−4; o, 0 to −4 ppm.

with the expected formation of hydrogen bonds from E7 and N2 to the E7 carboxyl.[33] The upfield shift of the T8 amide at higher pH's could also be rationalized as a destabilization of the hydrogen bond present at pH 2.2. However, similar destabilizations of C11 and Q16 amide donor bonds were not as strongly manifested in the small shifts observed. These values were similar to changes experienced by many other residues.

The large downfield shift of the Glu-7 and Asn-2 protons may be explained as partly due to the new hydrogen bond formation and partly due to electric field effects from the terminal amine as it approaches the two protons.[33] When the ionic strength of the solution was increased, a 1.1 ppm upfield shift was observed for N2, but no significant shift was observed for G7, whereas both the protons experienced the expected upfield shifts of 0.5 and 0.8 ppm, respectively. Most of the other protons and nitrogen signals shifted by less than 0.4 ppm. Exceptions included A9, which experienced a 1.0 ppm nitrogen shift, despite only 0.07 ppm shift in the proton signal, and A5, which changed by 0.7 and 0.17 ppm for nitrogen and proton signals, respectively.

It is clear that the presence of strong intramolecular hydrogen bonds does not consistently produce downfield shifts, as was suggested by comparative solvent studies on smaller peptides.

Torsion Angles. The relation between ^{15}N chemcial shifts and backbone torsion angles is, in the case of ω, due to the degree of delocalization of the nitrogen into the peptide bond, and for ϕ and Ψ, primarily the extent of nonbonded interactions. Although the allowed values for peptide torsion angles do not differ significantly between amino acids and proteins, it was expected that the relatively fixed values of these angles would allow perturbations of the amide nitrogen not observed in the averaged rotamers of the model compounds.

To a first approximation, large deviations of the peptide bond angle ω from 180° should be associated with upfield shifts from the random-coil models, due to decreased double-bond character. There are no data directly addressing the latter relationship; however, Llinas[6] reported ω angles from a crystal structure of aluminochrome along with ^{15}N chemical shifts. Chemical shift differences based on these data are not compatible with the expected trend and, in fact, show an opposite trend. We inspected the BPTI data in a similar fashion, using angle data from the x-ray structure of crystal form I.[28] A graph of $\Delta\delta^{15}N$ and the absolute value of the corresponding peptide angle ω shows a wide distribution of values for each angle.[54]

(54) Supplementary material, Figure s-3.

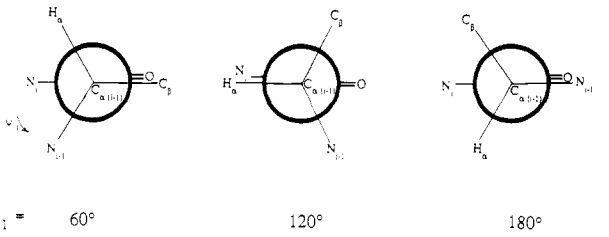

Figure 5. Projection of the C^{α}–C′ bond showing rotations of the Ψ angle. When Ψ is 180°, the nitrogen of residue $i-1$ eclipses the oxygen of the carbonyl attached to the observed nitrogen of residue i.

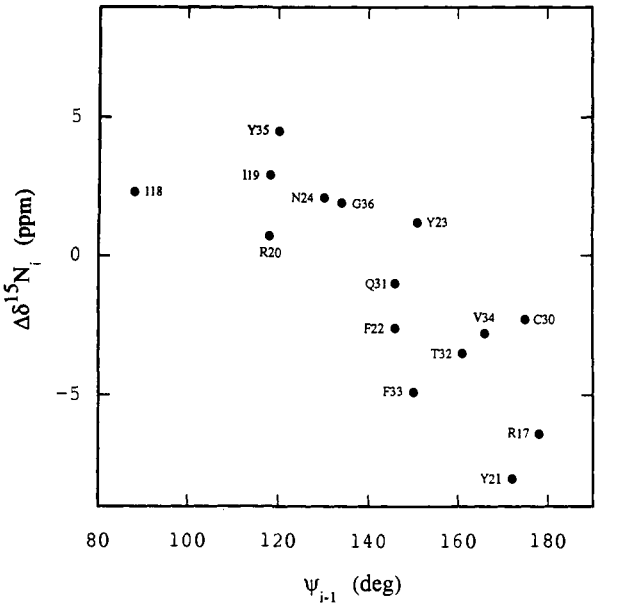

Figure 6. Plot of chemical shift differences, $\Delta\delta^{15}N$, for residues in the β-sheet region of BPTI against the Ψ angle of the preceding residue.

Similarly, the search for indications of systematic chemical shift changes, along with variations in the ϕ and Ψ angles, also produced no clear correlations.[55] Displaying four ranges of chemical shift differences on a Ramachandran plot of the ϕ and Ψ angles, for example, shows no obvious patterns (Figure 4).

The Ψ_{i-1} torsion angle for each residue was also examined in order to see the effects of steric interactions on the chemical shift of the ith nitrogen from groups on the preceding residue. Figure 5 shows the rotation about this bond and, in particular, the eclipsing of the carbonyl by the $(i-1)$th nitrogen at 180°. A plot of the $\Delta\delta^{15}N$ values of the ith residue against the Ψ_{i-1} angles shows an upfield shift from 120° to 180°.[56] When the residues are restricted to β-sheet residues, or subsets of the β sheet, the correlation is distinct (Figure 6). Residues not in the β sheet do not show as clear a correlation. This observation may reflect an effect between the C–N dipole and the C–O dipole of the $(i-1)$th residue, which would affect the delocalization of the ith nitrogen. It has been observed that large upfield shifts of carbonyl carbon atoms in cyclic ketones are caused by equatorial halogen substituents at the α position, and similar dipole interactions were suggested.[57]

Finally, some examples of χ^1 angles were inspected but appeared unrelated to chemical shift changes.

Other Nonbonded Effects. In addition to effects from neighboring substituents that are reflected torsion angles, other nonbonded interactions are possible between the amide group and other residues close in space. Though these perturbations are less systematic, and not well-defined,[10] they may be relevant in ex-

(55) Supplementary material, Figure s-4a,b.
(56) Supplementary material, Figure s-5.
(57) Metzger, P.; Casadevall, E.; Casadevall, A.; Pouet, M.-J. *Can. J. Chem.* **1980**, *58*, 1503–1511.

plaining the wider range of ppm shifts observed in folded peptides as compared to smaller flexible peptides. A detailed quantitative examination of van der Waals forces on particular amides was not possible, and so local regions around some residues were inspected for unusually bulky, polar, or aromatic groups, using the crystal structure II coordinates.[29]

In general, there is little in the crystal structure that indicates unusually different environments for residues with large chemical shift differences. For example, T8 and S47 have shift differences from their random-coil analogues of 14.9 ppm downfield and 14.7 ppm upfield, respectively. However, a 7-Å radius around each amide shows very similar environments in terms of distances from the nitrogens to aromatic groups, carbonyl groups, and other amides, although the S47 amide is in a more hydrophobic environment with less accessible surface area than the T8. Two arginine amides, R20 and R39, also differ in chemical shift by 13 ppm. In this case, the R20 amide nitrogen is within 3.5 Å of three carbonyls, whereas R39 is close to a cystine sulfur group. At present, these nearby structural elements cannot be used to rationalize the shifts, and more perturbing features such as nearby charged groups or unusually close aromatic groups are not observed. An extreme upfield shift of the G37 amide proton was measured by Tüchsen and Woodward[58] and attributed to strong ring current shifts, but this interesting case could not be investigated, due to lack of detectable signal in the heterocorrelated spectrum.

It is possible that solution structures will be more informative with regard to nonbonded interactions. In BPTI, for example, the solution structure reveals salt bridges that are not seen in the crystal.[31] These include the amides of R42, K46, and E49 directed toward various side-chain carboxyl groups. In this particular case, the amide resonances in question are all shifted upfield from their random-coil models, contrary to what might be expected from the apamin results. Other side-chain interactions, such as those involving van der Waals interactions, may produce important correlations if they can be quantified. At this stage, however, the constraints from NOE measurements are not sufficiently accurate to estimate these interactions. Inspection of the distance constraints for BPTI[31] does not reveal any bias in chemical shift as the number of amide proton constraints increases, reflecting the extent of close neighbors. This approach will be most beneficial in conjunction with molecular energy calculations that can provide estimates of van der Waals forces at each amide nitrogen.

In conclusion, an investigation of the empirical correlation between amide nitrogen chemical shifts and secondary structure in peptides and small proteins was undertaken. The different shifts did not show clear systematic variations with torsion angles, with the exception of a correlation to the Ψ_{i-1} angle observed for β-sheet amides of BPTI. The analysis of hydrogen bonding networks in BPTI also did not reveal any patterns, but downfield shifts of particular amides in apamin were observed as they formed hydrogen bonds. These results indicate that there is no single dominant effect but more likely a combination of factors that must contribute to the large chemical shift differences from random-coil models. These preliminary results suggest that the value of ^{15}N shifts for predicting detailed geometry may be limited. On the other hand, further investigation of the large chemical shift dispersion of these amides may contribute to the understanding of the nonbonded interactions that determine protein structures. Indeed, the lack of strong correlations of deviations of shifts to local torsion angles suggests that the deviations are not the result of local bonded variations but the summation of multiple nonbonded interactions.

Acknowledgment. Supported by NIH Grant GM-36596. Capital equipment was purchased with grants from NSF, NIH, and the Keck Foundation. We thank Bayer AG for the sample of BPTI (Trasylol).

Registry No. BPTI, 9087-70-1; apamin, 24345-16-2.

Supplementary Material Available: Figures illustrating variation of $\Delta\delta^{15}N$ for residues in BPTI, distributions of nitrogen chemical shift differences of BPTI amides for different classes of hydrogen-bonded amides and with variations in angle ω, a plot of ϕ_i and Ψ_i angles, and a plot of Ψ_{i-1} versus nitrogen chemical shift differences of residue i (7 pages). Ordering information is given on any current masthead page.

(58) Tüchsen, E.; Woodward, C. *Biochemistry* **1987**, *26*, 1918–1925.